

PAPER • OPEN ACCESS

Model for how an accretion disk drives astrophysical jets and sheds angular momentum

To cite this article: Paul M Bellan 2018 *Plasma Phys. Control. Fusion* **60** 014006

View the [article online](#) for updates and enhancements.

You may also like

- [The collision frequency of electron-neutral-particle in weakly ionized plasmas with non-Maxwellian velocity distributions](#)
Hong Wang, Jiulin Du and Rui Huo
- [Magnetohydrodynamic turbulence and turbulent dynamo in partially ionized plasma](#)
Siyao Xu and A Lazarian
- [Dynamics and chemical mode analysis of plasma thermal-chemical instability](#)
Hongtao Zhong, Mikhail N Shneider, Xingqian Mao et al.

Corrigendum: Model for how an accretion disk drives astrophysical jets and sheds angular momentum (2018 *Plasma Phys. Control. Fusion* **60** 014006)

Paul M Bellan 

California Institute of Technology, Pasadena CA 91125, United States of America

Received 1 November 2017

Accepted for publication 16 November 2017

Published 29 November 2017



CrossMark

The terms containing $\nabla \cdot (r^{-2}\nabla\psi)$ in equations (9a) and (9c) had the wrong sign in the paper ‘Model for how an accretion disk drives astrophysical jets and sheds angular momentum (2018 *Plasma Phys. Control. Fusion* **60** 014006)’. The corrected form of equation (9) is

$$\begin{aligned} \frac{\partial}{\partial t}(\rho U_r) + \nabla \cdot (\rho U_r \mathbf{U}) \\ = -\frac{1}{4\pi^2} \left(\frac{1}{\mu_0} \nabla \cdot \left(\frac{1}{r^2} \nabla \psi \right) \frac{\partial \psi}{\partial r} + \frac{\mu_0 I}{r^2} \frac{\partial I}{\partial r} \right) \\ - \frac{\partial P}{\partial r} + \frac{\rho U_\phi^2}{r}, \end{aligned} \quad (1a)$$

$$\frac{\partial}{\partial t}(\rho r U_\phi) + \nabla \cdot (\rho r U_\phi \mathbf{U}) = \frac{1}{4\pi^2} (\nabla I \times \nabla \psi \cdot \nabla \phi), \quad (1b)$$

$$\begin{aligned} \frac{\partial}{\partial t}(\rho U_z) + \nabla \cdot (\rho U_z \mathbf{U}) \\ = -\frac{1}{4\pi^2} \left(\frac{1}{\mu_0} \nabla \cdot \left(\frac{1}{r^2} \nabla \psi \right) \frac{\partial \psi}{\partial z} + \frac{\mu_0 I}{r^2} \frac{\partial I}{\partial z} \right) \\ - \frac{\partial P}{\partial z}. \end{aligned} \quad (1c)$$

Because the magnitude of the terms with the wrong sign was shown to be negligible in the discussion of equation (12) this incorrect sign has no impact on the discussion of the jet velocity as presented in section 4.1. However, the incorrect sign does have an impact on the jet collimation discussion presented in section 4.2. The ultimate result remains the same but the logical argument leading to this result needs to be corrected and in particular the argument given in equations

(25)–(27) needs to be replaced. This can be done in three equivalent and complimentary ways which will now be presented.

The first way is to restate equation (25) as

$$\begin{aligned} \frac{1}{\mu_0} \nabla \cdot \left(\frac{1}{r^2} \nabla \psi \right) &= \frac{\psi_0}{\mu_0 r^2} \frac{\partial^2}{\partial z^2} \left(\frac{1}{a(z)} \right)^2 \\ &= \frac{\psi_0}{\mu_0 a_0^2 r^2} \frac{\partial^2}{\partial z^2} \exp \left(-2 \int_0^z \kappa(z') dz' \right) \\ &= -2 \frac{\psi_0}{\mu_0 a_0^2 r^2} \frac{\partial}{\partial z} \left(\kappa(z') \exp \left(-2 \int_0^z \kappa(z') dz' \right) \right) \\ &= \frac{1}{\mu_0 r^2} \left(-2 \frac{\partial \kappa}{\partial z} + 4\kappa^2 \right) \psi \end{aligned} \quad (2)$$

so equation (26) with corrected sign becomes

$$-\frac{1}{\mu_0} \left[\nabla \cdot \left(\frac{1}{r^2} \nabla \psi \right) \right] \frac{\partial \psi}{\partial z} \sim \frac{1}{\mu_0 r^2} \left(2 \frac{\partial \kappa}{\partial z} - 4\kappa^2 \right) \psi \frac{\partial \psi}{\partial z}. \quad (3)$$

Since $\partial\psi/\partial z$ is negative, equation (3) provides a retarding force for sufficiently large $\partial\kappa/\partial z$ and this retarding force will overcome the accelerating force given in equation (27) if

$$2 \frac{\partial \kappa}{\partial z} - 4\kappa^2 > \lambda^2. \quad (4)$$

Thus retardation occurs if there is a sudden increase in κ which corresponds to a sharp turning of the poloidal field direction at the jet tip. Specifically, the poloidal field near the z axis is nearly in the z direction in the jet main body but at the jet tip turns abruptly to be in the r direction.

The second equivalent way is to note that there is a bunching up and hence greater density of poloidal flux surfaces at the jet tip. This occurs because the bundle of poloidal magnetic field lines that had been in the main jet body and aligned nearly parallel to the z axis turns to go in the positive

 Original content from this work may be used under the terms of the [Creative Commons Attribution 3.0 licence](https://creativecommons.org/licenses/by/3.0/). Any further distribution of this work must maintain attribution to the author(s) and the title of the work, journal citation and DOI.

r direction and then at larger r turns again to go in the negative z direction. This bunching up of poloidal field lines at the tip occurs because the jet distends what were initially dipole-like poloidal flux surfaces and stretches these flux surfaces out to the length of the jet. Thus, for a given r the poloidal flux is a slightly decreasing plateau going from $z = 0$ to the instantaneous length of the jet, while at the tip of the jet there is a cliff-like sudden fall-off of the poloidal flux from its plateau value to a much lower value in the vacuum-like region above the tip (i.e., region where z exceeds the jet length). The sudden fall-off region is where the distended poloidal field lines are bunched up. The greatly enhanced poloidal flux density in the cliff-like region implies that at the tip B^2 has a sharp local maximum with respect to z . The curvature term $-B^2\hat{R}/\mu_0R$ in equation (24) is large and points in the $-z$ direction at the hair-pin-like 180° turnaround of the bundle of poloidal field lines near the tip. For z slightly less than the location of maximum B^2 the gradient term $-\nabla_{\perp}(B^2/2\mu_0)$ is similarly large and also points in the $-z$ direction so the two terms on the right-hand side of equation (24) are additive and give a net retardation force at the tip. However, for z slightly larger than the location of maximum B^2 , i.e., just above the tip, the $-\nabla_{\perp}(B^2/2\mu_0)$ now points in the positive z direction whereas the curvature term $-B^2\hat{R}/\mu_0R$ continues to point in the negative z direction so above the tip

the curvature and gradient terms cancel rather than add. This is essentially a statement that the region above the tip has no current so the left-hand side of equation (24) vanishes, i.e., the curvature and gradient terms on the right-hand side of equation (24) are equal in magnitude and have opposite signs.

The third equivalent, but less precise way is to note that the squeezing together of the poloidal field lines in the main body near the z axis implies there is a positive J_{ϕ} while the turning of these field lines at the jet tip to go in the positive r direction implies that at the jet tip there is a positive B_r . The axial magnetic force component $-J_{\phi}B_r$ is thus negative and, if sufficiently large, will overcome the positive J_rB_{ϕ} magnetic force component and result in a retardation.

These arguments indicate that near the tip the jet slows down as was assumed in the remainder of section 4.2 which showed that such slowing down leads to a collimation of the jet.

Acknowledgments

Supported by USDOE Grant DE-FG02-04ER54755 (USDOE/ NSFPlasma Partnership).

Model for how an accretion disk drives astrophysical jets and sheds angular momentum

Paul M Bellan

California Institute of Technology, Pasadena CA 91125, United States of America

E-mail: pbellan@caltech.edu

Received 17 June 2017, revised 9 August 2017

Accepted for publication 14 August 2017

Published 12 October 2017



CrossMark

Abstract

Clumps of ions and neutrals in the weakly ionized plasma in an accretion disk are shown to follow trajectories analogous to those of fictitious ‘metaparticles’ having a charge to mass ratio reduced from that of an ion by the ionization fraction. A certain class of meta-particles have zero-canonical angular momentum and so spiral in towards the star. Accumulation of these meta-particles establishes a radial electric field that drives the electric current that flows in bidirectional astrophysical jets lying along the disk axis and provides forces that drive the jets. The entire process converts gravitational potential energy into jet energy while absorbing angular momentum from accreting material and shedding this angular momentum at near infinite radius.

Keywords: accretion disk, astrophysical jet, angular momentum, Hall MHD, dynamo, weakly ionized plasma, canonical angular momentum

(Some figures may appear in colour only in the online journal)

1. Introduction

This paper describes a model integrating the distinct physics of an accretion disk and bidirectional astrophysical jets as sketched in figure 1. The jets and disk form two physically separated regions which are part of the same electrical circuit and part of the same global magnetic field system. The disk serves as a mass source for the jets and powers the jets via a conversion of gravitational potential energy into an electromotive force (EMF) that drives a current flowing in a circuit passing through both the disk and the jets. Angular momentum is removed from the disk but not deposited in the jet. Instead the jet acts as a conduit through which angular momentum is transported to near infinite radius in the disk plane where it is shed with negligible associated energy exhaust. The first part of this paper describes the jet region

and while the second part describes the disk region and how the two regions connect to each other. An earlier version of this model containing quantitative estimates was provided in [1] and a more detailed version is given in [2].

1.1. Brief review of relevant previous work

Observational evidence strongly suggests that accretion disks and astrophysical jets are closely coupled and that disks act as the driver for jets. There is a large, rich literature on the topic of astrophysical jets and disks. We will not attempt to review this literature here other than mentioning a few relevant papers; a more extensive discussion of relevant literature is given in the introductions of [1] and [3]. There exists a variety of astrophysical jets which are distinguished by size and velocity. The smaller jets, called protostellar or Herbig–Haro jets, have a size of the order of the solar system, are non-relativistic and are associated with the early life of a star and the formation of planets. The larger jets are highly relativistic, have dimensions many orders of magnitude greater than protostellar jets, and are associated with black holes and neutron stars. A common feature



Original content from this work may be used under the terms of the [Creative Commons Attribution 3.0 licence](https://creativecommons.org/licenses/by/3.0/). Any further distribution of this work must maintain attribution to the author(s) and the title of the work, journal citation and DOI.

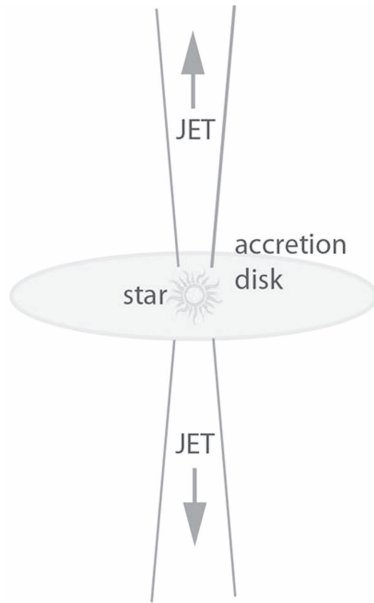


Figure 1. Bi-directional astrophysical jets originating from an accretion disk.

of all jets is that the jet is associated with an accretion disk and this feature suggests that existence of an accretion disk is a necessary condition for existence of a jet.

Most of the astrophysical literature addresses either disks or jets with relatively few papers discussing the coupling of disks to jets. In one of the earliest jet papers Blandford and Zjanek [4] proposed a model for the highly relativistic situation of a jet coming from a black hole. They assumed that magnetic flux was frozen into accreting material so that accretion would concentrate flux and that the disk was force-free. They noted the need for a radial electric potential drop in the disk plane and suggested there must be an effective finite resistivity to enable accreting material to cross magnetic field lines (i.e., not be frozen to the magnetic field). Their mechanism involved extracting energy from the rotation of the black hole to drive the jet.

The disk papers have primarily focussed on the magneto rotational instability (MRI). The original version of the MRI was presented by Balbus and Hawley [5] who assumed ideal MHD (i.e., Ohm's law given by $\mathbf{E} + \mathbf{U} \times \mathbf{B} = 0$ so there is zero resistivity) and a 100% ionized plasma undergoing Kepler rotation as the initial condition. Accreting particles contain angular momentum which must be shed because otherwise centrifugal force will reflect the particles at small radius. Classic viscosity in principle could transport angular momentum from small to large radius but the quantitative value of classical viscosity is negligible and so there has been a search for some non-viscous mechanism for transporting angular momentum outwards. The MRI papers argue that MRI turbulence provides the desired mechanism for outward transport of angular momentum in an accretion disk but generally do not address how disks drive jets. Blaes and Balbus [6] noted that protostellar accretion disks are weakly ionized so that the interaction between ions and neutrals would modify the MRI. Gammie [7] argued that if the ionization is very small, the effective resistivity

can become so large as to suppress the MRI and denoted regions where the ionization is negligible as 'dead zones'. Sano and Stone [8, 9] and Lesur [10] noted that the Hall term (which is missing from the ideal MHD equations used in [5–7]) becomes important when the disk is weakly ionized and affects the behavior of the MRI instability. The MRI investigations of the disk typically do not use the actual geometry but instead model a small portion of the disk where this portion, known as a shearing box, has an imposed velocity shear that mimics the radial dependence of the Kepler orbital velocity.

Jet models typically use ideal MHD and use the disk region as a boundary condition (this was done for example by Zhai *et al* [3]). However, a few papers such as those by Zanni *et al* [11], by Sheikhnezami *et al* [12], and by Stepanovs and Fendt [13] present models that couple disks and jets with the aim of showing how disks launch jets. These disk-jet coupling models invoked the ideal MHD equations for the jet and resistive MHD equations for the disk. The resistivity was made anomalously large and this enhancement in magnetic diffusivity was presumed to result from MRI turbulence. The value of the invoked anomalous resistivity was not calculated from first principles, but rather was chosen to provide plausible numerical results in numerical calculations. Furthermore, [11–13] did not take into account weak ionization or Hall physics.

Pandey and Wardle [14] considered the effect of the Hall term in a weakly ionized plasma from a more general point of view and noted that the effective ion cyclotron frequency is reduced by the fractional ionization which means that the effective ion cyclotron frequency can become very small. Since the cross-over from the MHD regime to the whistler regime occurs in the vicinity of the ion cyclotron frequency, they noted that weak ionization has the consequence of greatly lowering the frequency at which whistler waves occur.

Because the MHD equations have no intrinsic scale, these equations characterize situations ranging over many orders of magnitude and, in particular, the same dimensionless equations can characterize both a lab experiment and an astrophysical situation. A system for scaling from lab experiments to astrophysical situations was given by Remington *et al* [15] while Staff *et al* [16] noted '*the many similarities between laboratory jets and astrophysical jets despite the immense difference in scale speaks to the fundamental nature of the MHD jets*'. This similarity means that important insight into how jets work can be gained from studies of laboratory jets since, in principle, all aspects of laboratory jets can be controlled and all parameters can be measured. Jet lab experiments have been reported by Hsu and Bellan [17], You *et al* [18], Ciardi *et al* [19], Kumar *et al* [20], Suzuki-Vidal *et al* [21], Moser and Bellan [22], and Li *et al* [23].

1.2. Relation of the proposed model to previous models

The purpose of this paper is to present an integrated disk/jet model in the context of protostellar jets. This model does not depend on the MRI instability and so is fundamentally different from the MRI-based models because there is no invocation of turbulence or anomalous magnetic diffusivity. Furthermore, unlike the shearing box models typically used in

MRI models of disks, the geometry here is global and contains both the disk and the jet regions extending to infinity. The model depends on previously unrecognized particle kinetics and involves the new concept that a select group of particles have trajectories substantially different from Kepler or cyclotron motion. These trajectories are at the cross-over from Kepler to cyclotron orbits. A thought experiment indicating that such orbits must exist consists of imagining that a spacecraft slowly becomes electrically charged until its charge-to-mass ratio becomes the same as that of an ion. The spacecraft orbit would then have to change from being a Kepler orbit to being a cyclotron orbit and at the change-over there would have to be a trajectory that is neither Kepler nor cyclotron. Analysis shows that these special trajectories result from fundamental Hamiltonian orbit considerations missed when using the much coarser ideal MHD description. The existence of the group of particles having non-Kepler, non-cyclotron trajectories can equivalently be derived from the Hall MHD equations for a weakly ionized plasma.

2. Flux functions, fields, and currents

We assume axisymmetry and use a poloidal flux function ψ and a poloidal current I to prescribe the magnetic field

$$\mathbf{B} = \frac{1}{2\pi} \nabla \psi \times \nabla \phi + \frac{\mu_0 I}{2\pi} \nabla \phi \quad (1)$$

with an associated current density $\mathbf{J} = \mu_0^{-1} \nabla \times \mathbf{B}$. The field and current components are

$$\mathbf{B}_{\text{tor}} = \frac{\mu_0 I}{2\pi} \nabla \phi, \quad (2a)$$

$$\mathbf{B}_{\text{pol}} = \frac{1}{2\pi} \nabla \psi \times \nabla \phi, \quad (2b)$$

$$\mathbf{J}_{\text{tor}} = -\frac{r^2}{2\pi\mu_0} \nabla \cdot \left(\frac{1}{r^2} \nabla \psi \right) \nabla \phi, \quad (2c)$$

$$\mathbf{J}_{\text{pol}} = \frac{1}{2\pi} \nabla I \times \nabla \phi. \quad (2d)$$

The poloidal flux, the poloidal current, the disk region, and the jets are sketched in figure 2.

3. Motivation for the proposed model

The morphology of figures 1 and 2 consists of two regions: inside the disk and outside the disk. The interface between the two regions is indicated by the dotted ellipse in figure 2. The region outside the disk corresponds to the jet region and this region is what was modeled in Zhai *et al* [3] where the 3D MHD equations were solved numerically. The numerical solution in Zhai *et al* described a lab jet experiment at Caltech and also, by rescaling, an astrophysical jet. The numerical model required a scheme for injecting toroidal magnetic flux and this injection was accomplished in Zhai *et al* [3] by adding a fictitious source term (see equation 1(d) in Zhai *et al*) to the toroidal component of the induction

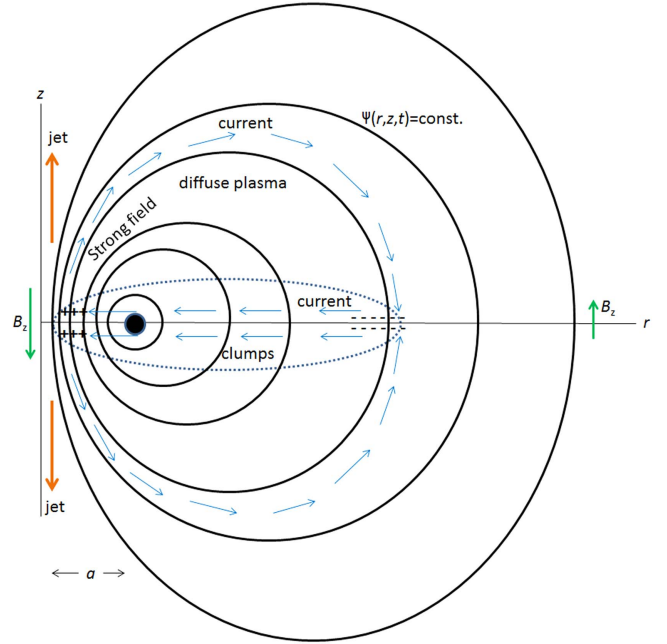


Figure 2. Jets are in $z > 0$ and $z < 0$ regions exterior to $z = 0$ plane while disk is in the $z = 0$ plane. The jets are governed by ideal MHD while the disk (inside dotted ellipse) is weakly ionized and is governed by Hall MHD and contains metaparticles making inward spiral trajectories. The black circle represents a toroidal current that creates the poloidal magnetic field (black curved lines). The electric circuit current is shown by the blue arrows. The poloidal magnetic field points down at small radius and up at large radius. This figure is reproduced with permission from [1].

equation; this fictitious source term was defined to be finite only near the base of the jet and so corresponded to injection of toroidal flux at the base of the jet. Without this fictitious source term toroidal flux would be conserved, but conservation of toroidal flux is contrary to what happens in a lengthening jet.

To see that flux conservation is contrary to what happens, consider that toroidal flux Φ in the jet scales as $\Phi \sim B_\phi a L(t)$ where a is the jet radius, $L(t)$ is the instantaneous jet length, and B_ϕ is the toroidal magnetic field in the jet. Although the toroidal flux is increasing, the poloidal current flowing in the jet and the associated B_ϕ in the jet are constant. Toroidal flux injection, i.e., non-conservation, is required because Φ increases as the jet lengthens; i.e., $d\Phi/dt \sim B_\phi a dL/dt$. Faraday's law mandates existence of a radial voltage drop $V = -d\Phi/dt$ at the jet base, and so there must be a radial electric field E_r at the jet base such that $V = -\int^r E_r dr$. The electric field and associated voltage drop can be considered as a battery-like EMF that drives the jet poloidal current with its associated toroidal magnetic field; in lab jet experiments this EMF is provided by an external power supply connected across inner and outer electrodes at the jet base. Because ideal MHD implies frozen-in magnetic flux, ideal MHD prohibits creation/injection of new toroidal flux so any model prescribing the EMF driving the jet current and its associated toroidal flux must lie outside the scope of ideal MHD.

Thus, the question is: how can toroidal flux be injected without resorting to insertion of a fictitious source term in the induction equation as was done in Zhai *et al* [3]? The jet interior and the jet dynamics are characterized by ideal MHD and the radial electric field E_r at the jet base is a boundary condition imposed where the jet interfaces with an accretion disk. Section 4 will describe the jet interior and jet dynamics. The mechanism for providing the EMF that injects toroidal flux at the base of the jet will then be presented in section 5 which describes behavior in the accretion disk.

4. Jets

4.1. Jet dynamics

The jet dynamics are governed by the ideal MHD equations

$$\rho \left(\frac{\partial \mathbf{U}}{\partial t} + \mathbf{U} \cdot \nabla \mathbf{U} \right) = \mathbf{J} \times \mathbf{B} - \nabla P, \quad (3a)$$

$$\frac{\partial \rho}{\partial t} + \nabla \cdot (\rho \mathbf{U}) = 0, \quad (3b)$$

$$\mathbf{E} + \mathbf{U} \times \mathbf{B} = 0, \quad (3c)$$

$$\nabla \times \mathbf{E} = -\frac{\partial \mathbf{B}}{\partial t}, \quad (3d)$$

$$\nabla \times \mathbf{B} = \mu_0 \mathbf{J}. \quad (3e)$$

Since the components of the convective derivative are

$$(\mathbf{U} \cdot \nabla \mathbf{U})_r = U_r \frac{\partial U_r}{\partial r} + U_z \frac{\partial U_r}{\partial z} - \frac{U_\phi^2}{r}, \quad (4a)$$

$$(\mathbf{U} \cdot \nabla \mathbf{U})_\phi = U_r \frac{\partial U_\phi}{\partial r} + U_z \frac{\partial U_\phi}{\partial z} + \frac{U_\phi U_r}{r}, \quad (4b)$$

$$(\mathbf{U} \cdot \nabla \mathbf{U})_z = U_r \frac{\partial U_z}{\partial r} + U_z \frac{\partial U_z}{\partial z}, \quad (4c)$$

on defining the total force $\mathbf{F} = \mathbf{J} \times \mathbf{B} - \nabla P$, the MHD equation of motion can be expressed as

$$\rho \left(\frac{\partial U_r}{\partial t} + U_r \frac{\partial U_r}{\partial r} + U_z \frac{\partial U_r}{\partial z} - \frac{U_\phi^2}{r} \right) = F_r, \quad (5a)$$

$$\rho \left(\frac{\partial U_\phi}{\partial t} + U_r \frac{\partial U_\phi}{\partial r} + U_z \frac{\partial U_\phi}{\partial z} + \frac{U_\phi U_r}{r} \right) = F_\phi, \quad (5b)$$

$$\rho \left(\frac{\partial U_z}{\partial t} + U_r \frac{\partial U_z}{\partial r} + U_z \frac{\partial U_z}{\partial z} \right) = F_z. \quad (5c)$$

The MHD continuity equation is

$$\frac{\partial \rho}{\partial t} + \frac{1}{r} \frac{\partial}{\partial r} (\rho r U_r) + \frac{\partial}{\partial z} (\rho U_z) = 0. \quad (6)$$

Adding U_r , U_ϕ , or U_z times equation (6) to the respective r , ϕ , or z component of equation (5) gives

$$\frac{\partial}{\partial t} (\rho U_r) + \nabla \cdot (\rho U_r \mathbf{U}) = F_r + \frac{\rho U_\phi^2}{r}, \quad (7a)$$

$$\frac{\partial}{\partial t} (\rho r U_\phi) + \nabla \cdot (\rho r U_\phi \mathbf{U}) = r F_\phi, \quad (7b)$$

$$\frac{\partial}{\partial t} (\rho U_z) + \nabla \cdot (\rho U_z \mathbf{U}) = F_z. \quad (7c)$$

Using $\mathbf{J} \times \mathbf{B} = \mathbf{J}_{\text{tor}} \times \mathbf{B}_{\text{pol}} + \mathbf{J}_{\text{pol}} \times \mathbf{B}_{\text{tor}} + \mathbf{J}_{\text{pol}} \times \mathbf{B}_{\text{pol}}$ the force vector can be expressed as

$$\mathbf{F} = \frac{1}{4\pi^2} \left[\frac{1}{\mu_0} \nabla \cdot \left(\frac{1}{r^2} \nabla \psi \right) \nabla \psi - \frac{\mu_0 I}{r^2} \nabla I - \nabla \phi \nabla \psi \cdot (\nabla I \times \nabla \phi) \right] - \nabla P \quad (8)$$

so equations (7a)–(7c) become

$$\begin{aligned} & \frac{\partial}{\partial t} (\rho U_r) + \nabla \cdot (\rho U_r \mathbf{U}) \\ &= \frac{1}{4\pi^2} \left(\frac{1}{\mu_0} \nabla \cdot \left(\frac{1}{r^2} \nabla \psi \right) \frac{\partial \psi}{\partial r} - \frac{\mu_0 I}{r^2} \frac{\partial I}{\partial r} \right) \\ & - \frac{\partial P}{\partial r} + \frac{\rho U_\phi^2}{r}, \end{aligned} \quad (9a)$$

$$\frac{\partial}{\partial t} (\rho r U_\phi) + \nabla \cdot (\rho r U_\phi \mathbf{U}) = \frac{1}{4\pi^2} (\nabla I \times \nabla \psi \cdot \nabla \phi), \quad (9b)$$

$$\begin{aligned} & \frac{\partial}{\partial t} (\rho U_z) + \nabla \cdot (\rho U_z \mathbf{U}) \\ &= \frac{1}{4\pi^2} \left(\frac{1}{\mu_0} \nabla \cdot \left(\frac{1}{r^2} \nabla \psi \right) \frac{\partial \psi}{\partial z} - \frac{\mu_0 I}{r^2} \frac{\partial I}{\partial z} \right) \\ & - \frac{\partial P}{\partial z}. \end{aligned} \quad (9c)$$

We now make the following simplifying, but realistic and relevant assumptions:

1. As in the derivation of the Grad–Shafranov equation [24, 25] we assume that $I = I(\psi)$ in which case $\nabla I \times \nabla \psi = 0$ so the current flows on and not across poloidal flux surfaces. This means that the right hand side of equation (9b) vanishes so there is no force in the ϕ direction. As discussed in [1] we assume $U_\phi = 0$ in the jet initially and since there is no force in the ϕ direction in the jet, U_ϕ will remain zero in the jet. The simplest nontrivial dependence is to have

$$\mu_0 I = \lambda \psi \quad (10)$$

which is closely related to force-free equilibria but not exactly the same because there is no assumption that the toroidal current is proportional to the toroidal flux.

2. We consider the geometry in figure 2 and in particular, assume that near the z axis, toroidal field pressure has stretched the poloidal magnetic field axially away from its original vacuum profile. The flux function ψ is assumed to be highly distended relative to its vacuum state so poloidal field lines near the z axis are nearly parallel to the z axis. The axial magnetic field $B_z = (2\pi r)^{-1} \partial \psi / \partial r$ is thus nearly uniform in the vicinity of the z axis; this uniformity corresponds to the requirement that near the z axis the poloidal flux must scale as r^2 to satisfy mathematical regularity. Because the axial field is nearly uniform near the z axis, if $a(z)$ is the assumed current channel radius, the

poloidal flux for $r \leq a$ can be approximated as

$$\psi(r, z) = \psi_0 \left(\frac{r}{a(z)} \right)^2, \quad (11)$$

where the dependence of a on z is weak so $\partial/\partial z \ll a^{-1}$. The poloidal field is assumed to have an umbrella- or mushroom-like shape with equation (11) describing the stalk only. At $z = 0$ this stalk intercepts what will be called the center electrode and so the center electrode has radius $a(0)$. At large distances the poloidal field bends around to form the cap of the mushroom and then returns back to the $z = 0$ plane at radii much larger than $a(0)$. This large radius part of the $z = 0$ plane will be called the outer electrode.

3. We assume $U_r \ll U_z$ and also that U_r is so small that it can be neglected.

Equations (9a)–(9c) are an exact re-statement of equation (3a) for an axisymmetric system. We seek a steady-state solution, i.e., a solution where $\partial/\partial t = 0$. and first note that for the poloidal flux specified by equation (11),

$$\nabla \cdot \left(\frac{1}{r^2} \nabla \psi \right) = \frac{\psi_0}{r^2} \frac{\partial^2}{\partial z^2} \left(\frac{1}{a(z)} \right)^2. \quad (12)$$

This shows that $\nabla \cdot (r^{-2} \nabla \psi)$ can be ignored compared to other terms in equations (9a) and (9c) because $\partial/\partial z$ is small compared to other terms. In equation (9c) the other terms are first order in $\partial/\partial z$ but the term involving $\nabla \cdot (r^{-2} \nabla \psi)$ is second order in $\partial/\partial z$ and so still can be dropped. The system is solved by considering the radial, azimuthal, and axial components of the equation of motion separately and then combining the results.

Radial component: Taking into account the assumptions $U_r \simeq 0$, $U_\phi = 0$, and using equation (10), equation (9a) becomes

$$0 = -\frac{1}{4\pi^2} \frac{\lambda^2 \psi}{\mu_0 r^2} \frac{\partial \psi}{\partial r} - \frac{\partial P}{\partial r} \quad (13)$$

which is essentially a balancing between the outward radial force from the pressure and the inward radial magnetic pinch force from $-J_z B_\phi$ since $J_z \sim r^{-1} \partial \psi / \partial r$ and $B_\phi \sim \psi / r$. Using equation (11), equation (13) can be expressed as

$$\frac{\lambda^2 \psi_0^2}{2\pi^2 \mu_0 (a(z))^4} r + \frac{\partial P}{\partial r} = 0 \quad (14)$$

which can be integrated using the boundary condition $P = 0$ at $r = a$ to give

$$P(r, z) = \frac{\lambda^2 \psi_0^2}{4\pi^2 \mu_0 (a(z))^2} \left(1 - \frac{r^2}{(a(z))^2} \right). \quad (15)$$

It should be noted here that the pressure given by equation (15) at $r = 0$ scales as $1/(a(z))^2$ and so is higher when $a(z)$ is smaller. This implies existence of an axial pressure gradient that will tend to drive flows from regions of small $a(z)$ towards regions of large $a(z)$.

Azimuthal component: Equation (9b) is satisfied because U_ϕ is assumed zero and $I = I(\psi)$ so $\nabla I \times \nabla \psi = 0$.

Axial component: Using $U_r \simeq 0$ and $U_\phi = 0$ equation (9c) becomes

$$\frac{\partial}{\partial z} (\rho U_z^2) = -\frac{\mu_0 I}{4\pi^2 r^2} \frac{\partial I}{\partial z} - \frac{\partial P}{\partial z} \quad (16)$$

which can be rearranged as a Bernoulli-like relation

$$\frac{\partial}{\partial z} \left(\rho U_z^2 + \frac{\mu_0 \lambda^2 \psi^2}{8\pi^2 \mu_0 r^2} + P \right) = 0. \quad (17)$$

On the z -axis $\psi^2/r^2 = 0$ and so on the z -axis equation (17) can be integrated to give the conventional Bernoulli relation

$$(\rho U_z^2 + P)_{r=0} = \text{const.} \quad (18)$$

Evaluation of $\rho(r, z)$, $U_z(r, z)$ and $P(r, z)$ on the z -axis axis at the two positions $z = 0$ and $z = L$ gives

$$\rho(0, 0) U_z^2(0, 0) + P(0, 0) = \rho(0, L) U_z^2(0, L) + P(0, L). \quad (19)$$

Next, assume that the axial position L is so large that $a(L) \gg a(0)$ and also assume that $U_z(0, 0)$ is nearly zero. This means that $\rho(0, 0) U_z^2(0, 0) \ll P(0, 0)$ and, since P scales as a^{-2} , that $P(0, L) \ll P(0, 0)$. Thus, equation (19) becomes

$$P(0, 0) = \rho(0, L) U_z^2(0, L). \quad (20)$$

From equation (15) it is seen that

$$P(0, 0) = \frac{\lambda^2 \psi_0^2}{4\pi^2 \mu_0 (a(0))^2} = \frac{\mu_0 I^2}{(2\pi a(0))^2} \quad (21)$$

so equation (20) can be solved to give

$$U_z(0, L) = \frac{1}{\sqrt{\mu_0 \rho(0, L)}} \frac{\mu_0 I}{2\pi a(0)}. \quad (22)$$

Equation (22) can also be expressed as

$$U_z(0, L) = \frac{B_\phi(0, a(0))}{\sqrt{\mu_0 \rho(0, L)}} \quad (23)$$

which is formally like the velocity of an Alfvén wave, but involves only B_ϕ rather than the total magnetic field $B = \sqrt{B_\phi^2 + B_z^2}$ and, furthermore, involves the magnetic field and the mass density evaluated at different locations.

The middle term in equation (17) is finite off the z axis and corresponds to the $J_r B_\phi \sim -\partial B_\phi^2 / \partial z$ axial force since $J_r \sim r^{-1} \partial \psi / \partial z$ and $B_\phi \sim r^{-1} \psi$. Equation (17) also shows that the generation of axial kinetic energy ultimately comes from $\partial a / \partial z$ being finite. This is because if a were independent of z then both ψ^2 and P would be independent of z and so there would be no axial force both on and off the z -axis.

Equation (22) has been verified experimentally at Caltech by Kumar and Bellan [20] who measured the time of flight of an MHD jet as a function of both current I and mass density ρ . Zhai *et al* [3] solved the MHD equations numerically for plasma parameters corresponding to the Caltech experiment and observed jet behavior consistent with the model presented here. The magnetically generalized Bernoulli relation given by equation (17) has been verified in the 3D numerical

simulation by Zhai *et al* [3] who observed that the local values at $r = a(z)$ of $\rho U_z^2 + B_\phi^2/(2\mu_0)$ remain constant with respect to change in z . The solutions in Zhai *et al* [3] were shown to scale to astrophysical jet parameters.

4.2. Jet collimation

The jet velocity increases with distance from the electrode so long as $a(z)$ is a weak function of z as discussed above. However, at the jet tip $a(z)$ is no longer a weak function of z because at the tip the poloidal magnetic field originating from the inner electrode bends over and goes back to intercept the outer electrode. Thus, the acceleration argument leading to equation (17) is no longer applicable. The bending over of the poloidal magnetic field results in a decelerating force that slows down the jet at the jet tip. This slowing down at the tip can be understood intuitively by recalling that the magnetic force can be decomposed as

$$\mathbf{J} \times \mathbf{B} = -\nabla_\perp \left(\frac{B^2}{2\mu_0} \right) - \frac{B^2}{\mu_0} \frac{\hat{\mathbf{R}}}{R}. \quad (24)$$

The first term, $-\nabla_\perp B^2/2\mu_0$, behaves like a pressure in the direction perpendicular to the magnetic field while the second term, $-\mu_0^{-1} B^2 \hat{\mathbf{R}}/R$, points in the direction opposite to the radius of curvature vector \mathbf{R} of the magnetic field and has magnitude inversely proportional to the radius of curvature. Suppose that the jet is extremely long and collimated in which case the poloidal field has a near hair-pin shape at the jet tip. Thus, a typical poloidal field line is approximately straight going from the inner electrode up to the jet tip and then reverses direction to return to the outer electrode. This reversal of poloidal field direction near the jet tip means there is a sharp 180° turn of the poloidal field at the jet tip. The radius of curvature of the poloidal field will thus be small at the jet tip but large elsewhere. Since the associated force scales inversely with R^{-1} and is directed in the $-\hat{\mathbf{R}}$ direction, there will be a strong retarding force at the jet tip but not elsewhere.

An equivalent way of looking at this development of a retarding force at the jet tip is to revisit the argument that $\sim \mu_0^{-1} [\nabla \cdot (r^{-2} \nabla \psi)] \partial \psi / \partial z$ can be dropped compared to $-r^{-2} \mu_0 I \partial I / \partial z$ in the axial force specified by the right hand side of equation (9c). Let us assume temporarily that $a = a_0 \exp(\int_0^z \kappa(z') dz')$ where $\kappa(z)$ is small and nearly independent of z for most of the jet length but then suddenly becomes large at the jet tip so as to provide the flaring out of the poloidal flux at the jet tip (the mushroom cap). With this assumption we express

$$\begin{aligned} \frac{1}{\mu_0} \nabla \cdot \left(\frac{1}{r^2} \nabla \psi \right) &= \frac{\psi_0}{\mu_0 r^2} \frac{\partial^2}{\partial z^2} \left(\frac{1}{a(z)} \right)^2 \\ &= \frac{\psi_0}{\mu_0 a_0^2 r^2} \frac{\partial^2}{\partial z^2} \exp \left(-2 \int_0^z \kappa(z') dz' \right) \\ &\sim 4 \frac{\kappa^2}{\mu_0 r^2} \psi + \dots \end{aligned} \quad (25)$$

so

$$\frac{1}{\mu_0} \left[\nabla \cdot \left(\frac{1}{r^2} \nabla \psi \right) \right] \frac{\partial \psi}{\partial z} \sim 4 \frac{\kappa^2}{\mu_0 r^2} \psi \frac{\partial \psi}{\partial z}. \quad (26)$$

By comparison, the term providing acceleration scales as

$$-\frac{\mu_0 I}{r^2} \frac{\partial I}{\partial z} = -\frac{\lambda^2 \psi}{\mu_0 r^2} \frac{\partial \psi}{\partial z} \quad (27)$$

so the retardation given by equation (26) will overcome the acceleration given by equation (27) when the flaring out of the poloidal flux is such that $\kappa(z) > \lambda/2$.

Being concentrated in the vicinity of the jet tip, the retarding force slows down the jet in the vicinity of the jet tip. An observer sitting in the jet frame near the tip would consequently see a converging axial velocity, i.e., a negative $\nabla \cdot \mathbf{U}$. The equation of continuity in the jet frame expressed as $\partial \rho / \partial t + \mathbf{U} \cdot \nabla \rho = -\rho \nabla \cdot \mathbf{U}$ implies that the plasma density seen by the observer in the jet frame increases where this local slowing occurs, much like traffic on a highway bunches up when a group of fast cars approaches a group of slower cars traveling in front of the fast cars. The axial compression of the jet plasma compresses the toroidal magnetic flux embedded in the jet plasma and this compression corresponds to increasing B_ϕ because B_ϕ is the density of toroidal flux. Since B_ϕ is what causes the pinch force, the bunching up of the fast jet approaching the slower jet at the tip increases pinching and so the jet becomes collimated. The radial pinching by axial deceleration can be seen quantitatively by first dotting the induction equation with $\nabla \phi$ to obtain

$$\nabla \phi \cdot \frac{\partial \mathbf{B}}{\partial t} = \nabla \phi \cdot \nabla \times (\mathbf{U} \times \mathbf{B}) \quad (28)$$

and then re-arranging equation (28) as

$$\begin{aligned} \frac{\partial}{\partial t} \left(\frac{B_\phi}{r} \right) &= \nabla \cdot [(\mathbf{U} \times \mathbf{B}) \times \nabla \phi] \\ &= \nabla \cdot \left[\mathbf{B} \frac{U_\phi}{r} - \mathbf{U} \frac{B_\phi}{r} \right] \\ &= \mathbf{B} \cdot \nabla \frac{U_\phi}{r} - \mathbf{U} \cdot \nabla \frac{B_\phi}{r} - \frac{B_\phi}{r} \nabla \cdot \mathbf{U}. \end{aligned} \quad (29)$$

Equation (29) is then recast to be in the jet frame as

$$\frac{d}{dt} \left(\frac{B_\phi}{r} \right) = \mathbf{B} \cdot \nabla \frac{U_\phi}{r} - \frac{B_\phi}{r} \nabla \cdot \mathbf{U}, \quad (30)$$

where d/dt denotes the convective derivative $\partial/\partial t + \mathbf{U} \cdot \nabla$, i.e., the time derivative seen by an observer in the jet frame. Since $U_\phi = 0$ was stipulated, equation (30) reduces to

$$\frac{d}{dt} \left(\frac{B_\phi}{r} \right) = -\frac{B_\phi}{r} \nabla \cdot \mathbf{U}. \quad (31)$$

However, the continuity equation can be written as

$$\frac{d\rho}{dt} + \rho \nabla \cdot \mathbf{U} = 0 \quad (32)$$

so elimination of $\nabla \cdot \mathbf{U}$ from equations (31) and (32) gives

$$\left(\frac{B_\phi}{r}\right)^{-1} \frac{d}{dt} \left(\frac{B_\phi}{r}\right) = \frac{1}{\rho} \frac{d\rho}{dt} \quad (33)$$

or

$$\frac{d}{dt} \ln\left(\frac{B_\phi}{r}\right) = \frac{d}{dt} \ln\rho \quad (34)$$

which leads to

$$\frac{B_\phi}{\rho r} = \text{const. in the jet frame.} \quad (35)$$

Thus axial compression increases ρ at a given r which causes a corresponding increase in B_ϕ and so an increase in pinching. Since the total current $I = 2\pi a B_\phi / \mu_0$ is a constant, the current channel radius a must decrease in the jet frame as B_ϕ increases. This reduction of a at the jet tip collimates the jet. The jet tip thus self-collimates and this self-collimation acts like a zipper continuously squeezing together poloidal field lines as the jet propagates. Because the flux tube is current-carrying, the magnetic field is helical and can be represented as $\mathbf{B} = B_\phi \hat{\phi} + B_z \hat{z}$. The jet flow is away from the region where the flux tube diameter is small and the jet flow direction remains the same when the current polarity is reversed. This is because the jet mechanism ultimately depends on the axial gradient of B_ϕ^2 which clearly is independent of the sign of B_ϕ and hence independent of the sign of the current.

The jet has a constant poloidal flux, but this flux is being axially distended since it is frozen into the jet. However, the toroidal flux in the jet is increasing because while B_ϕ is constant in the jet, the toroidal flux scales as the length of the jet. Thus, the linked toroidal and poloidal flux, i.e., the helicity, is increasing with time. The rate of helicity injection is proportional to the radial voltage drop at the electrodes driving the jet since this voltage corresponds to the rate of injection of toroidal flux. The jet requires a radial electric field to drive the poloidal current I and create the ever-increasing toroidal flux resulting from the lengthening of the jet. This radial electric field has been provided by a capacitor in laboratory experiments [17, 18, 22, 26] but obviously must be provided by other means in the situation of an accretion disk.

5. Accretion disk

5.1. Field and force symmetries

I and ψ are defined for both positive and negative z and, as sketched in figure 2, I is assumed to be an odd function of z while ψ is assumed to be an even function of z . Both I and ψ depend on r and both vanish at infinity. The disk lies in the $z = 0$ plane and is thin, weakly ionized, and in a Kepler orbit around a star. B_ϕ , B_r , and J_z are *antisymmetric* with respect to

z since $B_\phi \sim I$, $B_r \sim \partial\psi/\partial z$ and $J_z \sim \partial I/\partial r$ whereas $B_z \sim \partial\psi/\partial r$, $J_r \sim \partial I/\partial z$ and J_ϕ are *symmetric* with respect to z . The axial component of the magnetic force is thus *antisymmetric* with respect to z since

$$(\mathbf{J} \times \mathbf{B})_z = \underbrace{J_r}_{\text{symmetric}} \underbrace{B_\phi}_{\text{antisymmetric}} - \underbrace{J_\phi}_{\text{symmetric}} \underbrace{B_r}_{\text{antisymmetric}}, \quad (36)$$

whereas the radial component of the magnetic force is *symmetric* with respect to z since

$$(\mathbf{J} \times \mathbf{B})_r = \underbrace{J_\phi}_{\text{symmetric}} \underbrace{B_z}_{\text{symmetric}} - \underbrace{J_z}_{\text{antisymmetric}} \underbrace{B_\phi}_{\text{antisymmetric}}. \quad (37)$$

Because B_ϕ is antisymmetric with respect to z while B_z is symmetric, the $z > 0$ and $z < 0$ regions have opposite helicity magnetic fields so the total helicity of the entire system remains zero. The radial electric field E_r and the radial electric current J_r are oppositely directed in the $z = 0$ plane which indicates there is a power *source* in the $z = 0$ plane. This negative value of $\mathbf{E} \cdot \mathbf{J}$ in the disk (corresponding to the existence of a power *source*) is missing from models invoking anomalous resistivity (anomalously large magnetic diffusion) since increasing the resistivity corresponds to creating a *sink* for power and not a *source*. Since the disk is presumed to drive the jets, the disk should be a power *source* and the jets a power *sink*.

5.2. Inadequacy of ideal MHD Ohm's law to model accretion

The accretion disk is assumed to be in a Kepler orbit, i.e., at each radius the outward centrifugal force $\rho U_\phi^2/r$ is balanced by the inward gravitational force $\rho MG/r^2$ where M is the mass of the star and G is the gravitational constant so $U_\phi = \sqrt{MG/r}$, the Kepler orbital velocity. Previous astrophysical jet models have presumed that the accretion disk acts as a homopolar generator [27] in the presence of some pre-existing constant poloidal magnetic field, i.e., the B_z field threading the disk plane. According to this presumption, the Kepler rotation of the disk cuts the B_z field lines to create a radial electric field as prescribed by the ideal MHD Ohm's law equation (3c). The radial component of equation (3c) is

$$E_r + U_\phi B_z - U_z B_\phi = 0 \quad (38)$$

and because the anti-symmetry of the bidirectional jets mandates $U_z = 0$ in the $z = 0$ plane, equation (38) reduces to $E_r = -U_\phi B_z$ where U_ϕ is the disk's Kepler rotational velocity. Despite the intuitive appeal of this argument, it cannot be correct because if equation (3c) is to be invoked, then all components of equation (3c) must be satisfied, not just the radial component. The failure of equation (3c) becomes evident upon consideration of its azimuthal component, namely

$$E_\phi + U_z B_r - U_r B_z = 0. \quad (39)$$

The B_z magnetic field threading the $z = 0$ plane is assumed to be both constant in time and axisymmetric. The azimuthal electric field is $E_\phi = -r^{-1} \partial V / \partial \phi - \partial A_\phi / \partial t$. It is seen that E_ϕ must vanish in the $z = 0$ plane since axisymmetry implies $\partial V / \partial \phi = 0$ while B_z being constant in time implies $\partial A_\phi / \partial t = 0$. The anti-symmetry with respect to z of the jet

axial velocity implies $U_z = 0$ in the $z = 0$ plane. Because the jets are a bidirectional outflow of matter from the disk plane and because the configuration is in steady-state in the $z = 0$ plane, there must be a continuous radially inward flow of matter in the $z = 0$ plane to supply the matter continuously flowing out of the $z = 0$ plane in the bidirectional jets. This implies that U_r must be both finite and radially inwards in the $z = 0$ plane; i.e., there must be accretion. Because B_z is finite in the $z = 0$ plane, the term $-U_r B_z$ in equation (39) must be finite and yet no other term exists in equation (39) to balance this term (recall that $E_\phi = 0$ and $U_z = 0$ in the $z = 0$ plane). Thus, the disk cannot be governed by equation (3c) and so ideal MHD is an inadequate model for the accretion disk in contrast to ideal MHD being adequate for the jet region external to the accretion disk.

5.3. Kepler versus cyclotron orbits

We claim that a plasma cannot simultaneously satisfy the ideal MHD equations and be in a Kepler orbit [28]. To prove this claim we examine the distinction between Kepler and cyclotron motion in detail. In order to present the essential idea in the clearest possible fashion, we first restrict consideration to motion in the $z = 0$ plane and also assume the magnetic field is constant, uniform, and normal to the $z = 0$ plane. The magnetic field is then given by $\mathbf{B} = B_z \hat{z}$ with an associated azimuthal vector potential $A_\phi = B_z r/2$ and an associated poloidal flux $\psi = B_z \pi r^2$. We consider a particle having mass m and charge q in the gravitational field of a central object of mass M . The respective Lagrangian and Hamiltonian for the particle in the combined gravitational and magnetic field are

$$\mathcal{L} = \frac{1}{2}m(v_r^2 + r^2\dot{\phi}^2) + qr\dot{\phi}A_\phi + \frac{mMG}{r} \quad (40)$$

and

$$H = \frac{1}{2}m(v_r^2 + r^2\dot{\phi}^2) - \frac{mMG}{r}. \quad (41)$$

The canonical angular momentum defined as $P_\phi = \partial\mathcal{L}/\partial\dot{\phi}$ is

$$\begin{aligned} P_\phi &= mr^2\dot{\phi} + qrA_\phi(r) \\ &= mr^2\dot{\phi} + \frac{q}{2\pi}\psi(r). \end{aligned} \quad (42)$$

Lagrangian mechanics shows that because $\partial\mathcal{L}/\partial\phi = 0$, P_ϕ is a constant of the motion. An important consequence of the term containing $q\psi(r)$ in equation (42) is that a charged particle behaves very differently from a neutral particle. Equation (42) can be rearranged to give the angular velocity

$$\dot{\phi} = \frac{P_\phi - \frac{q}{2\pi}\psi(r)}{mr^2}. \quad (43)$$

On substituting equation (43) into (41) the Hamiltonian can be expressed as

$$H = \frac{1}{2}mv_r^2 + \chi(r), \quad (44)$$

where the effective potential $\chi(r)$ can be decomposed into two terms as

$$\chi(r) = \chi_\phi(r) + \chi_g(r). \quad (45)$$

The first term is the azimuthal kinetic energy $mv_\phi^2/2$ expressed as [28, 29]

$$\chi_\phi(r) = \frac{\left(P_\phi - \frac{q}{2\pi}\psi(r)\right)^2}{2mr^2} \quad (46)$$

while the second term

$$\chi_g(r) = -\frac{mMG}{r} \quad (47)$$

is the gravitational potential energy. If the particle is neutral so $q = 0$ then χ reverts to the classic Kepler form $\chi(r) = P_\phi^2/(2mr^2) - mMG/r$ which leads to circular Kepler orbits when r is at the minimum of $\chi(r)$. Using $\psi \sim B_z \pi r^2$, comparison of the orders of magnitudes of χ_ϕ and χ_g gives

$$\frac{\chi_\phi}{\chi_g} \sim \frac{q^2 B_z^2 r^3}{m^2 MG} = \frac{\omega_c^2}{\omega_K^2}, \quad (48)$$

where $\omega_c = qB_z/m$ is the cyclotron frequency and $\omega_K = \sqrt{MG/r^3}$ is the Kepler frequency. For typical astrophysical parameters, cyclotron frequencies are many orders of magnitude larger than the Kepler frequency so χ_ϕ is orders of magnitude larger than χ_g . This means that gravity is of negligible importance for charged particles and so charged particles will not execute Kepler orbits. If a plasma is fully ionized, all particles are either electrons or ions, no particle executes a Kepler orbit [28], and so the plasma center of mass cannot execute a Kepler orbit. Hence, it is not possible for a fully ionized ideal MHD plasma to be in a Kepler orbit. However, if the magnitude of ω_c were somehow reduced to become comparable to ω_K , the two effective potentials would then have associated forces of similar magnitude in which case the motion would differ substantively from either strict cyclotron or strict Kepler motion. This reduction of ω_c^2/ω_K^2 could be accomplished either by having a very weak magnetic field B_z or by having a very small charge to mass ratio q/m .

5.4. Weak ionization as a method for having an effective cyclotron frequency comparable to the Kepler frequency

Reduction of ω_c^2/ω_K^2 by having charged dust grains was considered in [30] and while this appears physically possible, it seems unlikely to be the typical situation. Instead, the effect of weak ionization appears to be a more likely means by which this reduction could occur because accretion disks rotating around new-born stars are very weakly ionized [7, 14] with fractional ionization ratios in the range $\alpha \sim 10^{-13}$ – 10^{-8} . The neutral particle density is quite high, nominally $n_n \sim 10^{16} \text{ m}^{-3}$. Because of the weak ionization, to a first approximation one can ignore the charged particles and

simply presume that the neutrals are in Kepler orbits around the star. Also, because there are α^{-1} more neutrals than charged particles, charged particles collide mainly with neutrals rather than with other charged particles. Assuming a nominal temperature of 100 K, the thermal velocity of neutrals is $v_{Tn} \sim 10^3 \text{ m s}^{-1}$ and so assuming a nominal atomic cross section $\sigma = 3 \times 10^{-20} \text{ m}^2$, the nominal neutral-neutral collision frequency will be $\nu_{nn} = \sigma n_n v_{Tn} = 0.3 \text{ s}^{-1}$ and collisions of an ion with a neutral will have a similar frequency. It is assumed that ion-neutral collisions are so frequent that ions collide with neutrals and scatter before completing a cyclotron orbit; this means that ions can be considered unmagnetized. On the other hand, because the electron cyclotron frequency is m_i/m_e times higher than the ion cyclotron frequency whereas the electron thermal velocity is only $\sqrt{m_i/m_e}$ times larger than the ion thermal velocity for equal electron and ion temperatures, regimes exist where the electrons *complete* a cyclotron orbit before being scattered by a collision. Thus, we are considering a regime [8, 31] where the electrons are magnetized but the ions are not. By ‘magnetized’ we mean that the particle completes a cyclotron orbit.

We now argue that despite the ions being unmagnetized, the *combination* of ions and neutrals behaves in the manner of a fictitious magnetized particle having a charge to mass ratio smaller than that of an ion by the fractional ionization α . To see this, consider a hypothetical situation where a transient electromagnetic force imparts a certain momentum to the ions during an interval shorter than the ion-neutral collision time. After acquiring this momentum, the ions collide with the neutrals and share this momentum with the neutrals. Because of this sharing, the combination of the ions and neutrals have the momentum the ions received from the electromagnetic force and the total mass of the ions and the neutrals. This shared momentum is identical to what would have been gained by a fictitious particle having the ion charge and a mass equal to the sum of the masses of the ions and neutrals under consideration and so a charge to mass ratio $\alpha q_i/m_i$ where α is the fractional ionization. Thus, the center of mass of the combination of ions and neutrals behaves like a fictitious ‘metaparticle’ having cyclotron frequency $\omega_c = \alpha q_i/m_i$; this reduction of effective cyclotron frequency was previously noted by Pandey and Wardle [14] who showed this would greatly lower the frequency at which whistler wave physics occurs since the cross-over from MHD physics to whistler physics occurs in the vicinity of the ion cyclotron frequency. Since $\alpha \sim 10^{-13}$ – 10^{-8} and ion cyclotron frequencies are typically 8–13 orders of magnitude larger than Kepler frequencies, metaparticles with a cyclotron frequency of the order of the Kepler frequency should exist in a typical accretion disk. Ionization is typically stratified [7] because α depends on ionization via x-ray or ultra-violet radiation, and so typically α varies from being essentially zero in the disk equatorial plane (as this plane is shielded by the disk particles from x-rays and UV) to being near unity at the interface between the disk face and the low-density, fully ionized plasma external to the disk. Thus, there will always be a disk stratum where α is such that the metaparticle cyclotron frequency is of the order of the Kepler frequency.

The time required for the neutrals to become collisionally attached to an ion can be estimated by considering a single ion and its associated α^{-1} neutrals (e.g. one ion and 10^{12} neutrals) and supposing that the ion receives some momentum from an electromagnetic field. The ion can be considered to constitute a delta-function momentum input which will collisionally diffuse through the surrounding α^{-1} neutrals. The volume occupied by the α^{-1} neutrals is $V = (\alpha n_n)^{-1}$ so the characteristic linear dimension of the clump of the α^{-1} neutrals is $l = V^{1/3} = (\alpha n_n)^{-1/3}$. The momentum diffusion coefficient is $D \sim v_T^2/\nu_{nn} = v_T/(\sigma n_n)$. The diffusion equation gives the time t_d to diffuse a length l as $l^2 \simeq 4Dt_d$ so

$$t_d = \frac{l^2}{4D} = \frac{\sigma n_n^{1/3} \alpha^{-2/3}}{4v_T} \quad (49)$$

which indicates times of the order of nanoseconds or less for the electromagnetic momentum gained by an ion to be shared via collisional diffusion with its associated α^{-1} neutrals assuming $\alpha \sim 10^{-13}$ – 10^{-8} . Thus, it is very reasonable to consider an ion and its associated α^{-1} neutrals to be collisionally attached to each other.

The metaparticle equation of motion can be derived in an alternative, equivalent, and more formal way by consideration of the MHD equation of motion for a weakly ionized plasma in a gravitational field, namely

$$\rho \frac{d\mathbf{U}}{dt} = \mathbf{J} \times \mathbf{B} - \nabla(P_i + P_e + P_n) - \rho \mathbf{g} \quad (50)$$

and the Hall Ohm’s law expressed in the form of the electron fluid equation of motion,

$$0 = n_e q_e (\mathbf{E} + \mathbf{u}_e \times \mathbf{B}) - \nabla P_e. \quad (51)$$

Electron collisions have been dropped from equation (51) since electrons are assumed magnetized so ω_{ce} exceeds the electron-neutral collision frequency. The gravitational force on electrons has also been dropped from this equation because the electron cyclotron frequency exceeds the Kepler frequency by many orders of magnitude. Using $\mathbf{J} = n_i q_i \mathbf{u}_i + n_e q_e \mathbf{u}_e$, subtraction of equation (51) from (50) yields

$$\rho \frac{d\mathbf{U}}{dt} = -n_e q_e \mathbf{E} + n_i q_i \mathbf{u}_i \times \mathbf{B} - \nabla(P_i + P_n) - \rho \mathbf{g}. \quad (52)$$

Since the plasma is weakly ionized, the overall mass density is essentially the neutral mass density, i.e., $\rho = n_n m_n$ where m_n is the mass of a neutral particle and n_n is the neutral particle number density. Dividing equation (52) by ρ and invoking the quasi-neutrality condition $n_e q_e = -n_i q_i$ yields

$$\frac{d\mathbf{U}}{dt} = \alpha \frac{q_i}{m_n} (\mathbf{E} + \mathbf{u}_i \times \mathbf{B}) - \frac{\nabla(P_i + P_n)}{n_n m_n} - \mathbf{g}. \quad (53)$$

Because the ions collide frequently with the neutrals, the mean ion velocity \mathbf{u}_i is nearly the center of mass velocity \mathbf{U} which is essentially the neutral center of mass velocity. The mean ion and center of mass velocities are presumed to be of order the Kepler velocity which at 1 a.u. is $3 \times 10^4 \text{ m s}^{-1}$. A hydrogen gas with nominal temperature of 100 K has a thermal velocity of the order of 10^3 m s^{-1} which is significantly lower than the Kepler velocity. Also, the direction

of rotation is assumed without loss of generality to be in the positive ϕ direction; or equivalently, the direction of Kepler rotation defines the positive ϕ direction. Finally, if the pressure term can be neglected on the basis that the random thermal velocities are small compared to the Kepler-like center of mass velocity, equation (53) reduces to

$$\frac{d\mathbf{U}}{dt} = \alpha \frac{q_i}{m_n} (\mathbf{E} + \mathbf{U} \times \mathbf{B}) - \mathbf{g} \quad (54)$$

which is the equation of motion for a metaparticle with charge to mass ratio $\alpha q_i/m_n$. Assuming the neutral mass is similar to the ion mass, the effective cyclotron frequency is thus reduced from the ion cyclotron frequency by α , i.e., by 10^{-13} – 10^{-8} . Ion-neutral collisions do not exist in equation (54) because the momentum ions lose from colliding with neutrals is precisely the momentum neutrals gain from these collisions and equation (54) describes the evolution of the sum of the ion and neutral momenta. Thus, ion-neutral and neutral-ion collisions have no effect on the metaparticle momentum. Instead, these collisions are the means by which the ions and neutrals are bound together to form the metaparticle. The metaparticle point of view is thus a type of two-fluid system where instead of having the two fluids being ions and electrons, now the two fluids are metaparticles and electrons.

A metaparticle is thus a clump of particles having effective charge to mass ratio $\alpha q_i/m_i$. Just as ion motion for phenomena slow compared to ω_{ci} can be described by the guiding center approximation (i.e., $\mathbf{E} \times \mathbf{B}$ drifts, polarization drifts, curvature drifts, and grad B drifts), the metaparticle motion can similarly be described by the guiding center approximation for phenomena slow compared to $\alpha \omega_{ci}$. However, if the Kepler frequency ω_K is comparable to the metaparticle cyclotron frequency $\alpha \omega_{ci}$, then the guiding center approximation cannot be used for metaparticles and a qualitatively different behavior occurs. An essential result of the guiding center approximation is that particles remain on poloidal magnetic flux surfaces to the extent that the $mr^2\dot{\phi}$ term in equation (42) is small compared to the $q\psi/2\pi$ term. However if $\omega_K \simeq \alpha \omega_{ci}$, the two terms in equation (42) become comparable, the guiding center approximation fails, and metaparticles can move across flux surfaces. In contrast to metaparticles, electrons remain governed by the guiding center approximation and so cannot move across magnetic flux surfaces. This distinction between metaparticle motion and electron motion leads to the possibility of a steady radial electric current composed of metaparticles, but not electrons, flowing across magnetic flux surfaces. The metaparticle constitutes the carrier of the radial current.

5.5. Inward spiral orbits of zero-canonical angular momentum particles

Equation (54) is the equation of motion for a charged particle with mass m_n and charge αq_i in a gravitational field and a magnetic field. The discussion can now be generalized by removing the four previously imposed restrictions that (i) motion is confined the $z = 0$ plane, (ii) the magnetic field is constant, (iii) the magnetic field is uniform, and (iv) there is

no electric field. With the removal of these restrictions the metaparticle Hamiltonian H generalizes to

$$\frac{H}{m_n} = \frac{1}{2}(\dot{r}^2 + r^2\dot{\phi}^2 + \dot{z}^2) - \frac{MG}{\sqrt{r^2 + z^2}} + \frac{\alpha q_i}{m_n} V(r, z, t), \quad (55)$$

where $V(r, z, t)$ is an electrostatic potential. Because the system remains axisymmetric, the canonical angular momentum is still a constant of the motion, i.e.,

$$P_\phi = m_n r^2 \dot{\phi} + \frac{\alpha q_i}{2\pi} \psi(r, z, t) = \text{const.} \quad (56)$$

On substituting for $\dot{\phi}$ using equation (56) the Hamiltonian assumes the form

$$\frac{H}{m_n} = \frac{1}{2}(\dot{r}^2 + \dot{z}^2) + \chi(r, z, t), \quad (57)$$

where the effective potential χ now is

$$\chi(r, z, t) = \frac{\left(\frac{P_\phi}{m_n} - \frac{1}{2\pi} \frac{\alpha q_i}{m_n} \psi(r, z, t) \right)^2}{2r^2} - \frac{MG}{\sqrt{r^2 + z^2}} + \frac{\alpha q_i}{m_n} V(r, z, t). \quad (58)$$

Now consider the special case where $P_\phi = 0$ and assume temporarily that $V = 0$ so the effective potential becomes

$$\chi(r, z, t) = \frac{\alpha^2 q_i^2 (\psi(r, z, t))^2}{m_n^2 8\pi^2 r^2} - \frac{MG}{\sqrt{r^2 + z^2}}. \quad (59)$$

Since B_z is approximately uniform at small r , the poloidal flux for small r is

$$\psi(r, x, t) = \pi B_z(0, z, t) r^2 \quad (60)$$

in which case

$$\chi(r, z, t) = \frac{\alpha^2 q_i^2 B_z^2(0, z, t) r^2}{m_n^2 8} - \frac{MG}{\sqrt{r^2 + z^2}}. \quad (61)$$

The radial force on the particle is $\mathbf{F} = -\partial\chi/\partial r$ and this force is always radially inwards because the radial partial derivative of both terms on the right hand side of equation (61) is positive. Thus, a particle is subjected to an inward radial force at any z . If the particle reaches $r = 0$ at finite z , the gravitational term provides an axial force towards the midplane $z = 0$. Thus, a particle will always experience a combination of forces directing it towards $r = 0, z = 0$, i.e., towards the central mass. The $P_\phi = 0$ assumption can be used in equation (56) to give

$$\dot{\phi} = -\frac{1}{2\pi r^2} \frac{\alpha q_i}{m_n} \psi(r, z, t) \quad (62)$$

so using equation (60)

$$\dot{\phi} = -\frac{1}{2} \frac{\alpha q_i}{m_n} B_z(0, z, t) \quad (63)$$

i.e., $\dot{\phi}$ is minus half the metaparticle cyclotron frequency. Suppose a metaparticle was initially orbiting at a radius r_0 with a Kepler frequency $\omega_K = \sqrt{MG/r_0^3}$ and that $P_\phi = 0$ was

satisfied at this initial radius. Because P_ϕ is a constant of the motion, P_ϕ will remain zero throughout the particle's entire motion. The combination of radially inward velocity and angular velocity $\dot{\phi} = -\alpha\omega_{ci}/2$ means the $P_\phi = 0$ metaparticle makes an inward spiral trajectory. This can be easily verified by solving equation (54) numerically with $P_\phi = 0$ set as an initial condition. Note that B_z must be negative at small r since we have assumed that $\dot{\phi}$ is positive; this corresponds to the downward direction of the magnetic field at small r in figure 2.

Since metaparticles have positive charge and spiral inwards, their accumulation near $r = 0$, $z = 0$ implies a build-up of positive charge near the origin and so the electrostatic potential V will become finite and there will be a radially outward electric field E_r . Metaparticle accumulation then is the mechanism for producing the radial electric field discussed in section 3. The concentration near $r = 0$ of positive charge from the accumulated metaparticles cannot be neutralized by electron motion in the $z = 0$ plane because electrons cannot move across poloidal flux surfaces. This constraint on electron motion results from conservation of the electron canonical angular momentum $P_\phi^e = m_e r^2 \dot{\phi} - e\psi(r, z, t)/2\pi$; noting that m_e is negligible $P_\phi^e = \text{const.}$ implies that $\psi(r, z, t)$ is conserved for an electron. Electrons therefore cannot deviate from their initial poloidal flux surface and so cannot move in the $z = 0$ plane to neutralize the accumulated positive charge of the inward spiraled metaparticles. However, as sketched in figure 2, electrons can move along constant ψ contours outside of the $z = 0$ plane and so can make their way from large r in the disk plane to small r in the disk plane by moving along a constant ψ surface. This electron motion out of the disk plane along constant ψ surfaces corresponds to a clockwise electric current in the region above the $z = 0$ plane and a counter-clockwise electric current in the region below the $z = 0$ plane. At small r , this poloidal electric current is axially outwards from the $z = 0$ midplane above and below the midplane. These poloidal currents produce a toroidal magnetic field into the page above the $z = 0$ plane and out of the page below the $z = 0$ plane. The topology of the current is precisely what is required to drive bidirectional jets away from the midplane.

Also, a portion of the inward spiraling metaparticles can serve as the feedstock for the jet mass flux. Since $U_\phi = r\dot{\phi}$ and $\dot{\phi}$ is constant for the inward spiraling metaparticles, the metaparticles have vanishing U_ϕ at small radius and so the assumption that the jet starts with $U_\phi = 0$ is seen to be reasonable.

5.6. Hall Ohm's law point of view

When the Hall term is included, the ideal MHD Ohm's law generalizes to be the Hall Ohm's law

$$\mathbf{E} + \mathbf{U} \times \mathbf{B} - \frac{1}{n_e e} \mathbf{J} \times \mathbf{B} = 0. \quad (64)$$

The addition of the Hall term $-\mathbf{J} \times \mathbf{B}/(n_e e)$ does not correspond to adding 'new' physics to the model but instead corresponds to correcting an over-simplification inherent in

ideal MHD. This over-simplification is the assumption in ideal MHD that the Hall term can be dropped because the difference between each component of the perpendicular electron and ion velocities is much less than the ion velocity component, i.e., ideal MHD is based on the assumption that

$$\left| \frac{J_k}{n_e e} \right| = |u_{ik} - u_{ek}| \ll |u_{ik}| \approx |U_k| \quad (65)$$

for each perpendicular component k . Specifically, for a magnetic field in the z direction, k would be the r or ϕ directions. The assumption prescribed by equation (65) is true if both the ion and electron perpendicular motions are dominantly $\mathbf{E} \times \mathbf{B}$ drifts. However the assumption prescribed by equation (65) is clearly false when there are inward spiraling metaparticles since ions, being constituents of the metaparticles, are spiraling in whereas the electrons, frozen to flux surfaces, are not. The entire radial electric current is thus produced by the radially inward ion velocity and so equation (65) is false because $u_{er} = 0$ causes equation (65) to imply $|u_{ir}| \ll |u_{ir}|$ which is clearly incorrect. An equivalent point of view is to consider the azimuthal component of equation (64), namely

$$-U_r B_z + \frac{1}{n_e e} J_r B_z = 0; \quad (66)$$

on dividing by B_z this becomes

$$J_r = n_e e U_r = \alpha n_n e U_r \quad (67)$$

which shows that the radial current comes from the metaparticles.

Because the Hall term in equation (66) is not contained in ideal MHD there is no term to balance the $-U_r B_z$ term in the azimuthal component. Inclusion of the Hall Ohm's law is effectively a tautology as it contains no physical information, but when the Hall term is omitted, the tautology is falsified. This is seen by noting that the Hall Ohm's law in the $z = 0$ plane is just the electron equation of motion for the situation where the electrons have no radial motion. The assumption in equation (65) which is the basis for ideal MHD, falsely assigns the electrons a radial motion comparable to the ion radial motion.

5.7. Accretion and removal of angular momentum via magnetic braking

An essential requirement for any accretion model is a mechanism for removing angular momentum of accreting mass. Suppose for the moment that the accreting mass is neutral so the effective potential is

$$\chi(r) = \frac{P_\phi^2}{2mr^2} - \frac{mMG}{r}. \quad (68)$$

If angular momentum were not removed, then as $r \rightarrow 0$ the $P_\phi^2/2mr^2$ contribution to the effective potential energy would diverge making it energetically impossible for accreting neutral material to attain arbitrarily small r . Because torque is the rate of change of angular momentum, removing angular momentum of accreting matter at some radial location r

means there must be a negative or ‘braking’ torque at this r . Magnetic forces can provide such a braking torque and the detailed mechanism can be understood in terms of conservation of canonical angular momentum or, equivalently, by consideration of the azimuthal component of the MHD equation of motion.

5.8. Braking torque from conservation of canonical angular momentum

Consider an axisymmetric magnetic field and its associated vector potential $rA_\phi(r, z, t) = \psi(r, z, t)/2\pi$ so conservation of canonical angular momentum is expressed as

$$P_\phi = mr^2\dot{\phi} + \frac{q}{2\pi}\psi(r, z, t) = \text{const.} \quad (69)$$

The time derivative of equation (69) for each species σ gives

$$0 = \frac{d}{dt}(m_\sigma r^2\dot{\phi}) + \frac{q_\sigma}{2\pi} \left(\frac{\partial\psi}{\partial t} + \frac{\partial\psi}{\partial r} \frac{dr}{dt} + \frac{\partial\psi}{\partial z} \frac{dz}{dt} \right), \quad (70)$$

where $d/dt = \partial/\partial t + \mathbf{v} \cdot \nabla$ is the time derivative experienced by an observer moving with a particle having velocity \mathbf{v} . Recalling that

$$B_r = -\frac{1}{2\pi r} \frac{\partial\psi}{\partial z}, \quad B_z = \frac{1}{2\pi r} \frac{\partial\psi}{\partial r}, \quad (71)$$

equation (70) can be expressed as

$$\begin{aligned} \frac{d}{dt}(m_\sigma r^2\dot{\phi}) &= -\frac{q_\sigma}{2\pi} \left(\frac{\partial\psi}{\partial t} + \frac{\partial\psi}{\partial r} \frac{dr}{dt} + \frac{\partial\psi}{\partial z} \frac{dz}{dt} \right) \\ &= -\frac{q_\sigma}{2\pi} \frac{\partial\psi}{\partial t} - q_\sigma r (B_z v_{r\sigma} - B_r v_{z\sigma}). \end{aligned} \quad (72)$$

Multiplying equation (72) by n_σ and summing over species gives

$$\begin{aligned} \sum_\sigma \left(\frac{d}{dt}(n_\sigma m_\sigma r u_{\sigma\phi}) - m_\sigma r u_{\sigma\phi} \frac{dn_\sigma}{dt} \right) \\ = -r B_z J_r + r B_r J_z \\ = r \hat{\phi} \cdot (\mathbf{J}_{\text{pol}} \times \mathbf{B}_{\text{pol}}). \end{aligned} \quad (73)$$

Summing $n_\sigma q_\sigma v_{r\sigma}$ and $n_\sigma q_\sigma v_{z\sigma}$ on the right hand side of equation (72) gives the current densities J_r and J_z . Summing $n_\sigma q_\sigma$ over species gives zero because of quasi-neutrality so no term involving $\partial\psi/\partial t$ survives the summation of equation (72) over species. The continuity equation for each species can be written as

$$\frac{dn_\sigma}{dt} + n_\sigma \nabla \cdot \mathbf{u}_\sigma = 0 \quad (74)$$

so equation (73) becomes

$$\sum_\sigma \left(\begin{aligned} &\frac{\partial}{\partial t}(n_\sigma m_\sigma r u_{\sigma\phi}) \\ &+ \mathbf{u}_\sigma \cdot \nabla(n_\sigma m_\sigma r u_{\sigma\phi}) \\ &+ m_\sigma r u_{\sigma\phi} n_\sigma \nabla \cdot \mathbf{u}_\sigma \end{aligned} \right) = r \hat{\phi} \cdot (\mathbf{J}_{\text{pol}} \times \mathbf{B}_{\text{pol}}). \quad (75)$$

When summing over species in the first term on the left-hand side, the random velocities sum to zero so what remains is the

mean velocity of the species. equation (75) then becomes

$$\frac{\partial}{\partial t}(\rho r U_\phi) + \nabla \cdot \sum_\sigma (m_\sigma r u_{\sigma\phi} n_\sigma \mathbf{u}_\sigma) = r \hat{\phi} \cdot (\mathbf{J}_{\text{pol}} \times \mathbf{B}_{\text{pol}}). \quad (76)$$

We may ignore electron mass since m_e is much smaller than the ion or neutral masses and note that the strong collisional coupling between ions and neutrals causes $\mathbf{u}_i \simeq \mathbf{u}_n \simeq \mathbf{U}$ so

$$\sum_\sigma (m_\sigma r u_{\sigma\phi} n_\sigma \mathbf{u}_\sigma) \simeq \sum_{i,e} (m_\sigma r U_\phi n_\sigma \mathbf{U}) = \rho r U_\phi \mathbf{U}. \quad (77)$$

Here any terms involving the squares of random velocities have been dropped because these would eventually give a pressure gradient in the ϕ direction, but because of the assumed azimuthal symmetry $\partial P/\partial\phi = 0$.

Because $\mathbf{B}_{\text{pol}} = (2\pi)^{-1} \nabla\psi \times \nabla\phi$, $\mathbf{J}_{\text{pol}} = (2\pi)^{-1} \nabla I \times \nabla\phi$, and $r\hat{\phi} = r^2 \nabla\phi$ the right hand side of equation (76) can be expressed as

$$\begin{aligned} r \hat{\phi} \cdot (\mathbf{J}_{\text{pol}} \times \mathbf{B}_{\text{pol}}) &= r(\hat{\phi} \times \mathbf{J}_{\text{pol}}) \cdot \mathbf{B}_{\text{pol}} \\ &= (2\pi)^{-1} r(\hat{\phi} \times (\nabla I \times \nabla\phi)) \cdot \mathbf{B}_{\text{pol}} \\ &= (2\pi)^{-1} r^2 (\nabla\phi \times (\nabla I \times \nabla\phi)) \cdot \mathbf{B}_{\text{pol}} \\ &= (2\pi)^{-1} \nabla I \cdot \mathbf{B}_{\text{pol}} \\ &= (2\pi)^{-1} \nabla \cdot (I \mathbf{B}_{\text{pol}}) \\ &= (2\pi)^{-2} \nabla \cdot (I \nabla\psi \times \nabla\phi). \end{aligned} \quad (78)$$

Finally, using equations (77) and (78), equation (76) assumes the form

$$\frac{\partial}{\partial t}(\rho r U_\phi) + \nabla \cdot (\rho r U_\phi \mathbf{U}) = \frac{1}{4\pi^2} \nabla \cdot (I \nabla\psi \times \nabla\phi) \quad (79)$$

which is identical to equation (9b).

If the right hand side of equation (79) were zero, then this equation would be a conservation equation for the angular momentum density $\rho r U_\phi$. However, the right hand side can be finite and so act as either a source or sink of angular momentum depending on whether it is positive or negative. Because the right hand side is in the form of a divergence and because both ψ and I must vanish at infinity, integration of equation (79) over volume up to infinity will result in there being no contribution from the right hand side. Thus, if there is a source of angular momentum over some subvolume, the divergence form of the right hand side of equation (79) shows that some other subvolume must absorb all the angular momentum produced by the source. Because the flux term $\nabla \cdot (\rho r U_\phi \mathbf{U})$ on the left-hand side of equation (79) also has the form of a divergence, integration over the entire volume up to infinity shows that all contributions from angular momentum flux will similarly cancel. The result is that the volume integral up to infinity of equation (79) gives

$$\int \rho r U_\phi d^3r = \text{const.} \quad (80)$$

so the total angular momentum is exactly conserved even though there can be local fluxes of angular momentum and

local sources or sinks, i.e., local torques from the $\mathbf{J} \times \mathbf{B}$ force.

The right hand side of equation (79) describes the torque associated with magnetic forces. This magnetic torque, a source/sink for angular momentum, provides a non-mechanical means for transporting angular momentum from one subvolume to another *spatially separated* subvolume. This transport of angular momentum to a distant location can be understood by writing the right hand side as

$$\frac{1}{4\pi^2} \nabla \cdot (I \nabla \psi \times \nabla \phi) = \frac{1}{4\pi^2} (\nabla I \times \nabla \psi) \cdot \nabla \phi \quad (81)$$

and examining $\nabla I \times \nabla \psi$. If surfaces of constant I coincide with surfaces of constant ψ then, as in the Grad–Shafranov equation, this means $I = I(\psi)$ so $\nabla I = I' \nabla \psi$ and $\nabla I \times \nabla \psi = 0$ so no magnetic torque exists, or equivalently there is no source or sink of angular momentum.

In figure 2 the constant I surfaces approximately coincide with the constant ψ surfaces in the regions above and below the $z = 0$ plane. This corresponds to the poloidal electric current flowing *along* the poloidal magnetic flux surfaces in the regions above and below the $z = 0$ plane. Thus, above and below the $z = 0$ plane the poloidal flux surfaces can be considered to behave as set of concentric insulated conductors carrying the poloidal electric current.

However, if surfaces of constant I do not coincide with surfaces of constant ψ there will be a source or sink of angular momentum. This happens in the $z \simeq 0$ disk region where the current is radial whereas the magnetic field is vertical. This means $\nabla \psi$ is horizontal while ∇I is vertical so $\nabla I \times \nabla \psi \neq 0$. Thus $-rJ_r B_z$ is finite in the $z \simeq 0$ disk region, i.e., torques exist in the disk region. However, while J_r is always radially inwards, B_z is negative at small r and positive at large r so the torque has opposite polarities at small and large r . This torque reversal can also be seen from the point of view of the poloidal flux function. In figure 2 ψ is negative everywhere and has a minimum at the black circle. In the $z = 0$ plane and to the left of this minimum, $\partial\psi/\partial r$ is negative corresponding to negative B_z while to the right of the black circle, $\partial\psi/\partial r$ is positive corresponding to positive B_z ; see the vertical arrows indicating B_z in figure 2.

The inward spiraling metaparticles constitute a radially inward electric current so J_r is negative in the $z \simeq 0$ disk region. Since both J_r and B_z are negative in the $z \simeq 0$ disk region to the left of the black circle, the first term in equation (73) causes $-rB_z J_r$ to be negative corresponding to a removal of angular momentum in this region. On the other hand B_z is positive to the right of the black circle in the $z \simeq 0$ disk region while J_r remains negative corresponding to a creation of angular momentum in the $z \simeq 0$ disk region to the right of the black circle. Angular momentum is consequently being transported from the left to the right. Unlike viscosity which transports angular momentum between adjacent regions, magnetic torque transports angular momentum to a spatially separated region. In particular, angular momentum is extracted by the magnetic torque from a small- r region and then deposited into a non-adjacent large- r region that is connected, not by geometric proximity, but instead by having

the same ψ flux surface. The connectivity occurs via electric current flowing along the flux surfaces in the region external to the $z \simeq 0$ disk region and there is no need for the angular momentum $mr^2\dot{\phi}$ to be finite in this external region.

To see this in more detail, consider two nearby flux surfaces labeled ψ_1 and ψ_2 , let V_{12} denote the volume of the toroidal shell between these two flux surfaces, and let $S_{1,2}$ denote the geometric surfaces associated with $\psi_{1,2}$. The rate of change of angular momentum due to magnetic torque in this toroidal shell is prescribed by integration over the volume of the shell, i.e.,

$$\begin{aligned} & \int_{V_{12}} \frac{1}{4\pi^2} \nabla \cdot (I \nabla \psi \times \nabla \phi) d^3r \\ &= \frac{1}{4\pi^2} \left(\int_{S_2} (I \nabla \psi \times \nabla \phi) \cdot d\mathbf{s} - \int_{S_1} (I \nabla \psi \times \nabla \phi) \cdot d\mathbf{s} \right) \\ &= 0, \end{aligned} \quad (82)$$

where the last line is zero because $d\mathbf{s}$ is parallel to $\nabla \psi$ on the respective geometric surfaces $S_{1,2}$ and because $I \nabla \psi \times \nabla \phi$ has no ϕ component so Gauss's law can be used without concern about the shell being doubly-connected. Equation (82) states that the angular momentum removed magnetically from the disk region between ψ_1 and ψ_2 at small radius (left of black circle) is deposited into the disk region between ψ_1 and ψ_2 at large radius (right of black circle). Thus, angular momentum is transported electrically along the flux surfaces from the inner region to the distant outer region.

This magnetic transport of angular momentum has an important consequence regarding energy. A flux surface passing through small r to the left of the minimum of ψ in the $z = 0$ plane (left of black circle) and passes through large r to the right of this minimum. Furthermore, the smaller the value of r is to the left for this intersection of the flux surface with the $z = 0$ plane, the larger the value of r is for the intersection to the right. Because the kinetic energy of angular momentum is $mv_\phi^2/2 = (mr^2\dot{\phi})^2/(2r^2)$, the kinetic energy of a certain amount of angular momentum scales as $1/r^2$. Thus, the energy required to create angular momentum at extremely large r is negligible compared to the energy absorbed on removing angular momentum at small r . This means that there is negligible energy cost in transporting angular momentum from small r to large r . While both angular momentum and azimuthal kinetic energy are removed from the same small r location, the creation of angular momentum and of energy do not occur at the same location. As will be argued below, the removed energy goes into driving the jet while the removed angular momentum is shed in the disk plane at extremely large r .

This transfer of angular momentum can be visualized by imagining the accretion disk to have a set of 'gear teeth' at small radius and another set of gear teeth at large radius. A DC electric *generator* engages the gear teeth at small radius and a DC electric *motor* engages the gear teeth at large radius. The rotating disk at small radius drives the generator and the load provided by the generator acts as a braking torque. At the same time, the motor at large radius spins up the plasma by an

infinitesimal amount at large radius to shed the angular momentum absorbed at small radius. Because angular momentum scales as $mr^2\dot{\phi}$ a tiny amount of angular velocity at large radius absorbs the angular momentum associated with finite $\dot{\phi}$ at small radius. The electrical circuit connecting the generator to the motor has one wire in the $z = 0$ plane and another wire arching out of the disk into the region above (or below) the $z = 0$ plane following the poloidal flux surfaces. Thus, angular momentum is transferred from the inner region (generator) to the outer region (motor) with no mechanical contact between the two regions.

The energy budget is seen by considering the poloidal flux surfaces as equivalent to an azimuthally symmetric set of wires rising out of the $z = 0$ plane and carrying electric currents flowing in the poloidal direction. At small radius, these currents will attract each other and thus squeeze the plasma between the wires to produce an axial pressure gradient. This axial pressure gradient accelerates plasma in the z direction and this acceleration of matter constitutes an energy sink; off the z -axis there is additional axial acceleration provided by the magnetic force $\hat{z} \cdot \mathbf{J} \times \mathbf{B} = J_r B_\phi - J_\phi B_r$. This force is dominantly given by the $J_r B_\phi$ term when the jet is nearly collimated so B_z is approximately uniform in which case J_ϕ is small. Because magnetic field is frozen into the plasma in the region external to the disk, the poloidal field is frozen into the jet and so is distended by the jet. This stretching of the poloidal field plus the increasing volume of toroidal field in the lengthening jet correspond to an increase of the magnetic energy in the region external to the disk. The energy extracted from the disk goes into the jet and its frozen-in magnetic field. Thus the angular momentum and gravitational potential energy of the accreting disk particles are absorbed at a single location (small radius region of the disk) but are not deposited at some other single location. The extracted energy is deposited at the jet location which is in the vicinity of the z -axis and away from the $z = 0$ plane; this deposited energy becomes the jet kinetic and magnetic energy. In contrast, the extracted angular momentum is deposited at near infinite radius in the vicinity of the $z = 0$ plane.

Maximum power coupling occurs when the load resistance equals the battery internal resistance and if this is so, the voltage at the battery terminals is half the open-circuit voltage. Bellan [1] showed that this situation was a stable operating point, i.e., any deviation would cause a heating or cooling of the disk that would change the disk internal resistance in such a way as to drive the system back to this operating point. Because the electrical resistivity in the disk results from collisions with neutrals rather than from Spitzer resistivity, the resistivity increases with temperature. Stability occurs because if the disk is at the operating point where the load resistance matches the internal resistance and there is a perturbation that increases the current, this will heat the disk and so increase the disk electrical resistance which will then reduce the current.

The open-circuit voltage occurs when the outward force of the electric field resulting from the accumulation of metaparticles at small radius balances the inward gravitational

force. This is because if the electric field balances gravity, there is no more radial infall of metaparticles and so no current, i.e., an open-circuit. Thus, the open-circuit electric field is given by

$$q_i E_r^{\text{open}} = \frac{\alpha^{-1} m_n M G}{r^2} \quad (83)$$

since a metaparticle has charge q_i and mass $\alpha^{-1} m_n$ where m_n is the mass of a neutral. Since the voltage under matched load is half the open-circuit voltage, the loaded electric field will be

$$E_r^{\text{loaded}} = \frac{\alpha^{-1} m_n M G}{2 q_i r^2}. \quad (84)$$

5.9. Source current for poloidal magnetic field

Now consider electrons and metaparticles at $r = a$, $z = 0$, i.e., at the center of the black circle in figure 2 where there is a magnetic field null. These particles will experience the inward pull of gravity, outward centrifugal force, and a force from the electric field. Thus, radial force balance for the electrons at the black circle is given by

$$\frac{m_e u_{\phi e}^2}{a} + q_e E_r^{\text{loaded}} = \frac{m_e M G}{a^2}, \quad (85)$$

whereas radial force balance for metaparticles at the black circle is given by

$$\frac{\alpha^{-1} m_n u_{\phi mp}^2}{a} + q_i E_r^{\text{loaded}} = \frac{\alpha^{-1} m_n M G}{a^2}. \quad (86)$$

On substituting for E_r^{loaded} the electron and metaparticle toroidal velocities are prescribed by

$$u_{\phi e}^2 = \frac{M G}{a} \left(1 + \frac{\alpha^{-1} m_n}{2 m_e} \right), \quad (87)$$

$$u_{\phi mp}^2 = \frac{M G}{2 a} \quad (88)$$

which shows that the toroidal velocity of the metaparticles is slower than the Kepler velocity whereas the toroidal velocity of the electrons is much faster than the Kepler velocity. This is because gravity is aided by the electric force for electrons and opposed by the electric force for metaparticles. Assuming that both electrons and metaparticles are moving in the positive ϕ direction, the net toroidal current would then be negative and this would produce a poloidal magnetic field with the sense shown in figure 2. The electron motion is essentially a balance between the radially inward force from the electric field and the outward centrifugal force. The value of α at $r = a$, $z = 0$ will in general not be the same as for the metaparticles having zero-canonical angular momentum and the situation might be complicated by electron-neutral collisions that tend to dissipate the toroidal current and by capture of new particles that would tend to enhance the current. However, despite these complications there would tend to be a difference between electron and metaparticle toroidal velocities and hence a current that produces the poloidal magnetic field.

6. Summary

The global model presented here integrates the different physics of a weakly ionized accretion disk and the fully ionized region exterior to the disk. The exterior region contains bi-directional jets emanating from the accretion disk and powered by the accretion disk. A radial electric field in the accretion disk drives the jet poloidal current. The interaction between this current and its associated toroidal magnetic field provide the forces that drive and collimate the jets. The radial electric field can also be considered as the provider of the increasing amount of toroidal flux in the jets where this increase occurs because the jet length is continuously increasing. The radial voltage drop associated with this radial electric field is, as stipulated by Faraday's law, the rate of increase of toroidal flux in the jet. The radial electric field results from an accumulation of electric charge from a special group of accreting clumps of ions and neutrals, called metaparticles, that have a specific charge to mass ratio which causes the clump to have an inward spiral trajectory. This trajectory differs from both Kepler and cyclotron orbits and results from Hamiltonian dynamics that is missed using conventional MHD equations but can be deduced from consideration of Hall dynamics in a weakly ionized plasma in combined gravitational and magnetic fields. Electrons are not allowed to move across magnetic flux surfaces but can move on magnetic flux surfaces. Because electrons try to move in such a way as to maintain quasi-neutrality, the electrons move along flux surfaces in the external region in a fashion so as to try to cancel the build-up of positive charge resulting from accumulation of spiraled-in metaparticles. The consequence of the radial inward motion of the metaparticles in the disk plane and the radial inward motion of the electrons on flux surfaces out of the disk plane is to produce oppositely directed toroidal magnetic fields above and below the disk plane. This is the toroidal magnetic field responsible for jet acceleration and collimation. The process removes angular momentum from accreting mass and sheds this angular momentum at near infinite radius in the disk plane. Gravitational potential energy is absorbed from the accreting material and goes into powering the jets. The jets and their associated electric circuit act as a conduit for angular momentum but not as an absorber of angular momentum, just like copper wires act as a conduit for electric power but not as an absorber for electric power. Unlike models based on the MRI there is no turbulent instability involved.

The model presented here has been presented in much more detail in [1] and in particular, section 9 of [1] provides quantitative parameters for the situation of a protoplanetary disk and associated jet. This analysis provides self-consistent quantitative values for accretion mass influx rate, jet velocity,

jet ejection to accretion ratio, jet velocity, magnetic fields, ionization fraction, density, and temperature.

Acknowledgments

Supported by USDOE Grant DE-FG02-04ER54755 (USDOE/NSF Plasma Partnership).

References

- [1] Bellan P M 2016 *Mon. Not. R. Astron. Soc.* **458** 4400–21
- [2] Bellan P M 2017 *Magnetic Helicity, Spheromaks, Solar Coronal Loops, and Astrophysical Jets* (London: Imperial College Press) in preparation
- [3] Zhai X, Li H, Bellan P M and Li S T 2014 *Astrophys. J.* **791** 40
- [4] Blandford R D and Znajek R L 1977 *Mon. Not. R. Astron. Soc.* **179** 433
- [5] Balbus S A and Hawley J F 1991 *Astrophys. J.* **376** 214
- [6] Blaes O M and Balbus S A 1994 *Astrophys. J.* **421** 163
- [7] Gammie C F 1996 *Astrophys. J.* **457** 355
- [8] Sano T and Stone J M 2002 *Astrophys. J.* **570** 314
- [9] Sano T and Stone J M 2002 *Astrophys. J.* **577** 534
- [10] Lesur G, Kunz M W and Fromang S 2014 *Astron. Astrophys.* **566** A56
- [11] Zanni C, Ferrari A, Rosner R, Bodo G and Massaglia S 2007 *Astron. Astrophys.* **469** 811
- [12] Sheikhezami S, Fendt C, Porth O, Vaidya B and Ghanbari J 2012 *Astrophys. J.* **757** 65
- [13] Stepanovs D and Fendt C 2016 *Astrophys. J.* **825** 14
- [14] Pandey B P and Wardle M 2008 *Mon. Not. R. Astron. Soc.* **385** 2269
- [15] Remington B A, Drake R P and Ryutov D D 2006 *Rev. Mod. Phys.* **78** 755
- [16] Staff J E, Koning N, Ouyed R, Thompson A and Pudritz R E 2015 *Mon. Not. R. Astron. Soc.* **446** 3975
- [17] Hsu S C and Bellan P M 2002 *Mon. Not. R. Astron. Soc.* **334** 257
- [18] You S, Yun G S and Bellan P M 2005 *Phys. Rev. Lett.* **95** 045002
- [19] Ciardi A, Ampleford D J, Lebedev S V and Stehle C 2008 *Astrophys. J.* **678** 968
- [20] Kumar D and Bellan P M 2009 *Phys. Rev. Lett.* **103** 105003
- [21] Suzuki-Vidal F *et al* 2011 *Astrophys. Space Sci.* **336** 41
- [22] Moser A L and Bellan P M 2012 *Nature* **482** 379
- [23] Li C K *et al* 2016 *Nat. Commun.* **7** 13081
- [24] Grad H and Rubin H 1958 *Proc. 2nd UN Conf. on the Peaceful Uses of Atomic Energy* vol 31, p 190
- [25] Shafranov V D 1966 *Rev. Plasma Phys.* **2** 103
- [26] Yun G S and Bellan P M 2010 *Phys. Plasmas* **17** 062108
- [27] Valone T 1994 *The Homopolar Handbook* (Washington, DC: Integrity Research Institute) p 24
- [28] Bellan P M 2007 *Phys. Plasmas* **14** 122901
- [29] Schmidt G 1979 *Physics of High Temperature Plasmas* (New York: Academic) pp 29–44
- [30] Bellan P M 2008 *Astrophys. J.* **687** 311
- [31] Wardle M 1999 *Mon. Not. R. Astron. Soc.* **307** 849